



OPEN

Proton conduction of polyAMPS brushes on titanate nanotubes

SUBJECT AREAS:
SURFACES, INTERFACES
AND THIN FILMS
POLYMERSJun Feng¹, Yaqin Huang¹, Zhengkai Tu¹, Haining Zhang^{1,2}, Mu Pan^{1,2} & Haolin Tang^{1,2}¹State Key Laboratory of Advanced Technology for Materials Synthesis and Processing, Wuhan University of Technology, Wuhan 430070, China, ²Key Laboratory of Fuel Cell Technology of Hubei Province, Wuhan University of Technology, 430070, China.Received
27 March 2014Accepted
16 July 2014Published
29 August 2014Correspondence and
requests for materials
should be addressed to
H.N.Z. (haining.
zhang@whut.edu.cn)
or H.L.T. (thln@whut.
edu.cn)

Proton conducting materials having reasonable proton conductivity at low humidification conditions are critical for decrease in system complexity and improvement of power density for polymer electrolyte membrane fuel cells. This study shows that polyelectrolyte brushes on titanate nanotubes formed through surface-initiated free radical polymerization exhibit less humidity-dependent proton conduction because of the high grafting density of polymer electrolyte chains and well-distribution of ionic groups. The results described in this study provide an idea for design of new proton conductors with effective ion transport served at relatively low humidification levels.

Proton conducting materials have attracted considerable attention because of their promising applications as electrolytes in proton exchange membrane fuel cells (PEMFCs)^{1,2}. The commonly used and commercially available electrolyte materials for PEMFCs are perfluorosulfonated ionomers which composed of a poly(tetrafluoroethylene) backbone and fluorocarbon side-chains terminated with sulfonic acid groups³⁻⁵. For perfluorosulfonated ionomer membranes, although the exact microstructure is still in argument, it is well accepted that hydrophilic ionic channels for proton transportation are formed in the membrane through micro-phase separation induced by the hydrophobic fluorocarbon backbone and hydrophilic sulfonic acid end groups on the side chain of ionomers^{3,6}. The expansion and interconnection of the ionic channels by penetration of water molecules are generally required for effective proton transport in the membrane since the shrinkage or collapse of ionic channels induced by dehydration of the membrane could increase the proton transport resistance. Thus, fuel cells assembled from perfluorosulfonated membranes required humidification systems to keep the membrane electrolyte humidified which in turn can decrease the power density and increase the cost of the system⁷. To overcome the limitation of perfluorosulfonated membranes, many efforts have been devoted to organic-inorganic hybrids as alternative solid proton conducting electrolytes as discussed in recent topical reviews⁸⁻¹⁰. In particular, grafting of organic or polymeric electrolytes on porous materials provides enhanced thermal and chemical stability, improved water retention ability, and according proton conductivity at low relative humidity^{11,12}. This has led our attention to polymer electrolyte brushes bearing large density of sulfonic acid groups on hygroscopic matrix.

Herein, we show that polymer electrolyte brushes can effectively transport protons under less humidified conditions in a model system using poly(2-acrylamido-2-methylpropanesulfonic acid) (polyAMPS) as polymer electrolyte. Titanate nanotube (TiNT) is selected as matrix for immobilization of polymers since surface hydroxyl groups on TiNT provide easy accessibility for modification¹³ and good proton conduction at the surface¹⁴. In the formed polymer electrolyte brush system, one end of polymer chain is chemically attached to the solid substrate and the swelling of attached polymer chains in humid environment mainly occurs perpendicular to the substrate. The confined structure of attached polymer chains and the short distance between two anchored sites render the relative humidity required for water saturation relatively low, leading to low percolation threshold for proton transport in polymer electrolyte brushes. As a result, polymer electrolyte brush can reach high proton conductivity under low relative humidity conditions.

Results

The designed polyelectrolyte brushes were formed through in situ free radical polymerization (“grafting from” approach) thermally initiated by surface-attached initiator monolayer, as schematically shown in Figure 1a. The azobisisobutyronitrile (AIBN) type initiators were first immobilized on TiNT surface through coupling reaction of mono-chlorosilane end-groups of the initiator with surface hydroxyl groups. Sodium 2-acrylamido-2-methylpropane-sulfonate was chosen as model monomer for polymerization since the sulfonate group can be easily

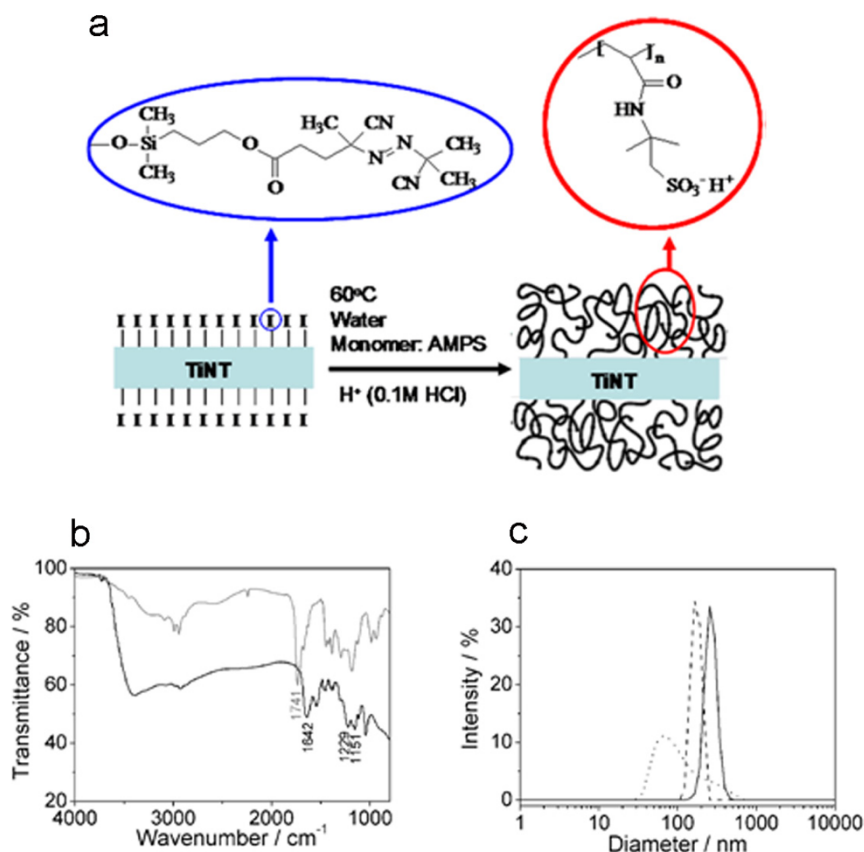


Figure 1 | Synthesis and characterization of polyAMPS brushes. (a) Synthesis of polyAMPS brushes. The AIBN type initiator monolayer was first self-assembled on the surface on TiNTs. The polyAMPS chains were directly grown from the surface by thermal initiation with the presence of monomers. (b) FTIR spectra were recorded for initiator (grey) and polyAMPS (black) attached TiNTs. PolyAMPS brush was formed by polymerization at 60°C for 6.5 hours. (c) Size distribution curves of free polyAMPS from solution (dash line), titanate nanotubes (dot line), and polyAMPS brushes on titanate nanotubes (solid line) were obtained from dynamic light scattering. Concentrations of the formed suspension solutions are 0.1 g ml⁻¹.

transferred to acid form and the bulk polymer in H⁺ form exhibited reasonable proton conductivity under certain humidification levels^{15,16}. It should be noted that, although the atom transfer radical polymerization provides precise control over the chemical composition and architecture, the possible residue of copper ions used as catalyst during polymerization process may affect the proton transportation process in the formed membranes¹⁷. Thus, traditional free radical polymerization was chosen for the growth of polyelectrolyte brushes.

To qualitatively determine whether the polyAMPS chains were successfully attached to TiNTs, FTIR spectra of samples before and after polymerization for 6.5 hours were recorded, as shown in Figure 1b. The clearly observed absorption bands at 1741 cm⁻¹ and 2240 cm⁻¹ for the sample before polymerization are assigned to the ester groups and cyano groups on initiator molecules, indicating that the initiator molecules were successfully attached to the surface of TiNTs. After polymerization, new absorption bands were observed at 1642 cm⁻¹, 1229 cm⁻¹, and 1151 cm⁻¹, attributed to C=O of amide, symmetric stretching mode of SO₃⁻, and anti-symmetric stretching mode of SO₃H groups on the monomer units, respectively. Thus, it can be concluded that the polyAMPS chains are successfully grafted onto the surface of TiNTs.

The TiNT substrates used for grafting of polyelectrolyte have the inner diameter of 5 nm, wall thickness of about 1.4 nm, and the Brunauer–Emmett–Teller (BET) surface area of 321 m² g⁻¹ calculated from adsorption-desorption isotherms, as reported in our previous work¹⁸. After surface initiated polymerization for 6.5 hours, grafting density of about 7.2 g of polyAMPS per gram of TiNT was

observed. The weight average molecular mass of surface attached polyAMPS was 3.03 × 10⁵ g mol⁻¹ as detected by gel permeation chromatography of free polymers in solution that has similar molecular weight with surface-attached polymers¹⁹. Assuming all the grafted polyAMPS located at the outer surface of TiNT, the distance between two surface-attached polyAMPS molecules can be estimated to be 3.7 nm and the dry layer thickness of grafted polyAMPS monolayer is about 31 nm considering the geometric parameters of TiNT (outer surface area of 196 m² g⁻¹). The high grafting density induced confined structure leads to locally ordered structure of surface-attached polyAMPS chains, which in turn may facilitate proton hopping along the polymer chain or between ionic sites in neighboring chains.

The homogeneity of the grafted polyelectrolyte may affect the interfacial properties and according proton transporting process for the formed membranes. Size distribution curves of free polyAMPS from solution, polyAMPS grafted and unmodified TiNTs in water with concentration of 0.1 g ml⁻¹ determined by dynamic light scattering measurements are displayed in Figure 1c. Although two peaks with hydrodynamic radius of about 80 and 280 nm corresponded to single TiNT and aggregation of TiNTs were observed for unmodified TiNTs, only one relatively narrow distributive peak at about 264 nm appeared for polymer electrolyte grafted TiNT. In addition, no aggregation was observed for polyelectrolyte grafted TiNTs suspension over one week due to the strong electrostatic repulsive forces of sulfonic acid segments whereas even precipitation can be clearly observed for unmodified TiNTs in one week. The well distribution of polyelectrolyte grafted TiNT suggests that

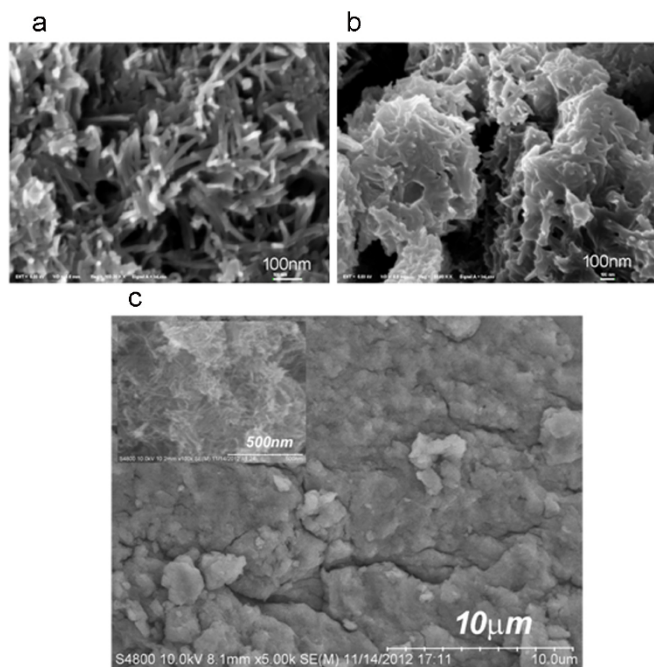


Figure 2 | SEMs image of synthesized samples. (a) SEM image of TiNTs prepared via hydrothermal process. (b) SEM image of powder sample of polyAMPS brushes on TiNTs (polymerization time 6.5 hours). (c) Cross-sectional SEM image of compacted pellet of polyAMPS brush. Sample was compacted to the pellet under 20 MPa pressure for 3 minutes. From the high resolution image (insert), TiNTs can be observed.

polymers are homogeneously attached to surfaces of all TiNTs since the grafting density has significant influence on swollen thickness of polymer electrolyte brushes²⁰. This could minimize the interfacial resistance of proton transportation in the following formed membrane.

Figure 2 shows scanning electron micrographs of synthesized TiNT powders, polyAMPS grafted TiNT powders, and cross-sectional image of polyAMPS brushes after compact to pellet which is about 1 cm in diameter and 1.4 mm in thickness. It can be clearly seen that TiNTs were fully covered with polymers after polymerization and the morphology of TiNT still remains. For the compacted pellet, the clearly observed interface can increase the proton transport resistance, suggesting that the proton conductivity values of the bulk material might be higher than that of the measured pellet.

The proton conductivity of polyAMPS brush with polymerization time of 6.5 hours were calculated from the electrochemical impedance spectra which were measured by sandwiched the compacted pellet between two gold electrodes in a homemade testing chamber. Figure 3a displays the original hodographs of impedance of polyAMPS brush at 60°C under different relative humidity. Although the exact value of proton conductivity relies on calculation, qualitative conclusion can be drawn by visual inspection of the impedance spectra, i.e the proton conductivity increased dramatically with the increase in relative humidity from 0% to 30% and it remained almost constant with further increase in relative humidity. Figure 3b shows the through-plane proton conductivity values of polyAMPS brushes pellet at 60°C under various humidification levels. Proton conductivity under the same conditions for pristine polyAMPS or physical mixture of polyAMPS and TiNTs was plotted in the same figure. It can be clearly seen that the proton conductivity of polyAMPS brush increased from $1.28 \times 10^{-3} \text{ S cm}^{-1}$ to $5.21 \times 10^{-3} \text{ S cm}^{-1}$ with increasing relative humidity from 0% to 30%. However, with further increase in relative humidity, the proton conductivity slightly increased, reaching $6.11 \times 10^{-3} \text{ S cm}^{-1}$ at relative

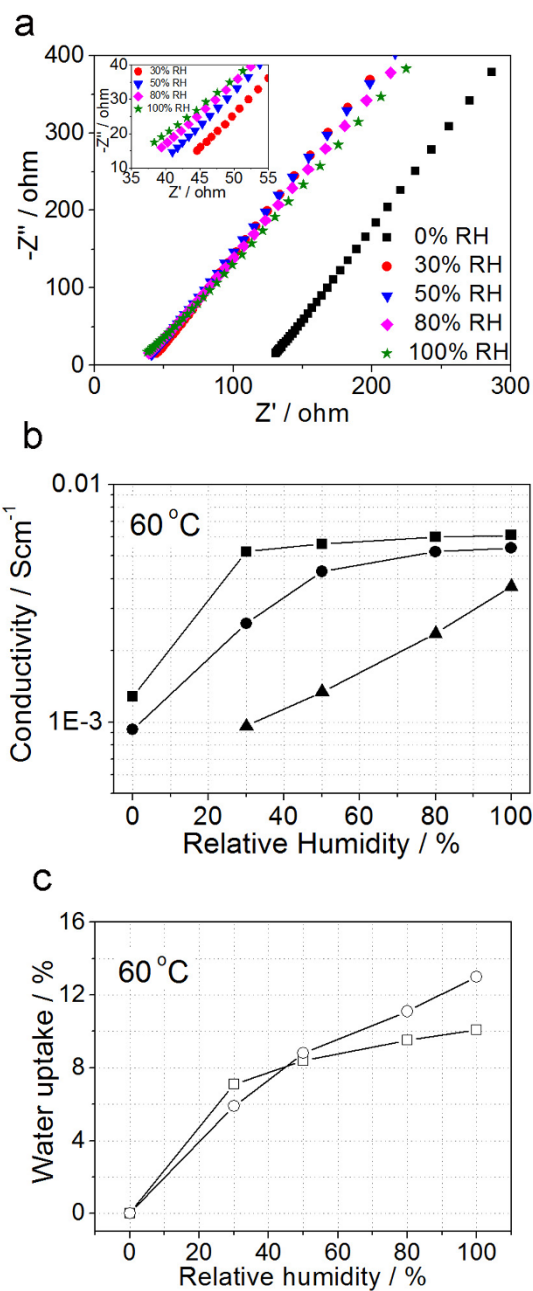


Figure 3 | Proton conductivity and water uptake of the formed samples. (a) Electrochemical impedance spectra of polyAMPS brush (polymerization time of 6.5 hours) under different humidity as indicated in the figure. (b) Calculated humidity-dependent proton conductivity of polyAMPS brush (solid squares, polymerization time of 6.5 hours), physically mixed polyAMPS and TiNTs (solid circles), and free polyAMPS (solid triangles). (c) Water uptake properties of polyAMPS brush (open squares, polymerization time of 6.5 hours) and free polyAMPS (open circles) under different relative humidity at 60°C. Relative humidity was controlled by added desired amount of water into the testing chamber and monitored with a humidity sensor. Solid lines are guide to eyes.

humidity of 100%. Although similar trend of humidity-dependant proton conductivity was observed for physically mixed sample of polyAMPS and TiNTs, the relative humidity of about 60% was required for water saturation, attributed to the weak electrostatic interaction between sulfonic acid groups on polymer chains and surface hydroxyl groups on TiNTs as observed in a similar system consisting of metal oxide and perfluorosulfonated ionomers in lit-

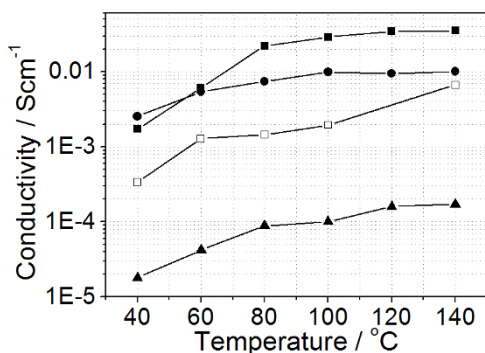


Figure 4 | Temperature dependent proton conductivity. Temperature dependent proton conductivity of polyAMPS brush (solid squares, polymerization time of 6.5 hours), physically mixed PolyAMPS and TiNTs (solid circles), and pure TiNTs (solid triangles) under 100% relative humidity. Open squares represent the proton conductivity of polyAMPS brush under anhydrous state at different temperatures. Solid lines are guide to eyes.

eratures²¹. Moreover, since water molecules can continuously swell pristine polyAMPS in three dimensions, the proton conductivity of pristine polyAMPS sample exhibits continuous increase with the increase in relative humidity. The above mentioned hypothesis of water saturation of polyAMPS was confirmed by water uptake ability of polyAMPS brush and pristine polyAMPS, as shown in Figure 3c. It can be clearly seen that the water uptake of polymer pellet made from free polyAMPS almost linearly increases with the increase in relative humidity up to 100% RH whereas the water uptake of polyAMPS brush increases slightly with the increase in relative humidity above 30% RH. Although the uptake of water for free polyAMPS is higher than that of polyAMPS brush under relative humidity above 50% RH, the proton conductivity of free polyAMPS is much lower than that of polyAMPS brush. It should be further mentioned that the proton conductivity of polyAMPS brush is much higher than that of pristine polyAMPS membrane in all tested humidification levels. This could be attributed to the locally ordered ionic groups induced by confined structure of polymer chains that can reduce the proton transporting resistance.

The temperature-dependent proton conductivity of polyAMPS brush under both hydrated and dry conditions is presented in Figure 4. As comparison, the proton conductivity values of pristine TiNTs membrane and membrane containing physical mixture of polyAMPS and TiNTs with thickness of about 80 μm under hydrated conditions were plotted in the same figure. The proton conductivity of polyAMPS brush increases with the increase in temperature for both humidification conditions, reaching the maximum proton conductivities of $3.51 \times 10^{-2} \text{ S cm}^{-1}$ under hydrated state and of $6.68 \times 10^{-3} \text{ S cm}^{-1}$ under dry state at 140°C , respectively. This can be understood since the migration of sulfonic acid segments and associated protons in the membrane become fast with the increase in temperature, leading to rapid proton transport and according high proton conductivity. However, it is of interest to note that the proton conductivity of polyAMPS brush is relatively high at dry conditions while considering that the proton transport generally requires water molecules to be involved and the proton conductivity for perfluorosulfonated ionomer membranes²² and pristine polyAMPS membranes are not detectable at the same condition. This result is in great contrast to polyAMPS grafted mesoporous silica materials, where the proton conductivity at low humidification levels is about 2–3 orders of magnitude lower than that in the system reported here under very similar conditions as physically adsorbed water evaporates with temperature¹¹. Although the mechanism of proton conduction for polyAMPS brush at dry state is not defined yet, the strong water-holding capacity by chemisorption of unreacted

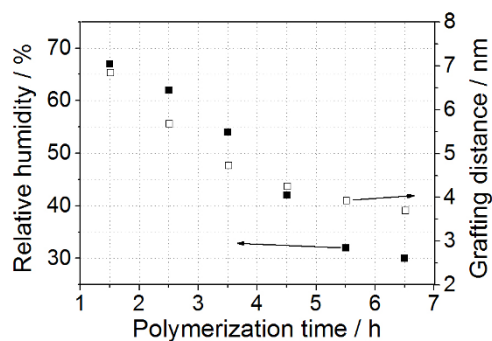


Figure 5 | Minimum relative humidity for water saturation in polyAMPS brushes. Effect of polymerization time for formation of polyAMPS brushes on minimum relative humidity (solid squares) for water saturation and grafting distance between neighboring polymer chains (open squares). Both minimum relative humidity and grafting distance decrease with increasing polymerization time.

surface hydroxyl groups and aqueous-like interface of TiNT may play crucial roles on dry state proton transport^{14,23,24}.

Discussion

The humidity-dependent conductivity of polyAMPS brush is in great contrast to that for perfluorosulfonated ionomer membranes reported in literature where proton conductivity significantly increases with increasing relative humidity even at high humidification levels^{4,22}. These different behaviors in proton conductivity for perfluorosulfonated ionomer membranes and polymer electrolyte brushes are likely attributed to microstructure of membranes, especially the distribution of sulfonic acid groups. To facilitate proton transport in perfluorosulfonated ionomer membranes, relative humidity above 80% is typically required for making the ionic channels induced by micro-phase separation expanded and interconnected²². In the case of polyAMPS brush, the confined structure of polymer chains induced by the short distance between two anchor sites results in one-dimensional swelling of polymer chains in the presence of water molecules. It is therefore expected that polyAMPS brushes can be saturated with water molecules at low relative humidity (below 30%) and exhibit less humidity-dependent proton conductivity compared to perfluorosulfonated ionomer membranes. This hypothesis was further proved with understanding the effect of grafting density of polymer chains on the proton conductivity of polyAMPS brushes.

Figure 5 shows the relative humidity to saturate polyAMPS brushes with water and grafting distance between two anchored sites of polymer chains as a function of polymerization time. The grafting distance was calculated based on the grafted amount and average molecular weight of synthesized polymers and surface area of TiNTs substrate. With the increase in polymerization time, more initiator moieties start to decompose and more polymer chains grow from surface of TiNTs. Accordingly, the grafting distance between neighboring polymer chains decreased with the increase in polymerization time, leading to the decreased free volume inside the polymer brushes. Therefore, less water molecules are required to saturate the polymer brushes with the increase in polymerization times, i.e. low percolation threshold for proton conduction was observed for polyAMPS brushes. It is worthy to be mentioned that, although the maximum proton conductivity of polyAMPS brush is lower than that of perfluorosulfonated ionomer membranes ($\sim 0.1 \text{ S cm}^{-1}$)²², proton conductivities of polyAMPS brush at relative humidity below 60% are higher than those of perfluorosulfonated ionomer membranes under same conditions ($10^{-4} - 4 \times 10^{-3} \text{ S cm}^{-1}$), demonstrating the potential application of polyelectrolyte brushes as electrolytes for less humidified fuel cell applications which can simplify the water



management during further fuel cell operation and improve the power density of fuel cells²⁵.

In summary, model proton conductor based on polyelectrolyte brushes in situ grown from titanate nanotube substrates has been prepared. The short grafting distance between two neighboring polymer chains lead to low relative humidity required for water saturation in polymer brushes. The results present here demonstrate that polymer electrolyte brushes on titanate nanotubes are promising less humidity-dependent proton conductors which can be used as additives in fuel cell electrolytes or as electrolytes for other electrochemical micro-device applications. Although this work focused on proton conduction, it might also be applied for other ion transport systems, for example lithium ion transportation.

Methods

Materials. Sodium 2-acrylamido-2-methylpropane sulfonate, hexachloroplatinic acid, laevulinic acid, and allyl alcohol were purchased from Alfa Aesar. Phosphorous pentachloride, potassium cyanide, and triethylamine were received from Kermel Chemical Reagent Ltd. (Tianjin, China). Titanium dioxide powder (P25) was purchased from Evonik Degussa, Germany. Toluene was distilled under a nitrogen atmosphere from sodium using benzophenone as an indicator. Water was deionized through a Milli-Q system (Barnsted Nanopore, resistivity = 18.0 MΩ cm⁻¹). All the other solvents and chemicals were reagent grade and were used as received. The initiator, dimethylchloro-silylpropyl 4-isobutyronitrile-4-cyano pentanoate was synthesized according to literatures^{20,26}. The TiNT substrates were prepared via hydrothermal process. The detailed synthetic process and characterization of TiNTs were reported elsewhere¹⁸.

Self-assembly of initiator on titanate nanotubes. To a suspension of TiNT (1 g) in anhydrous toluene (50 ml), a solution of initiator (1 g) in anhydrous toluene (20 ml) was added under an atmosphere of nitrogen. Triethylamine (1 ml) was added to the mixture as catalyst for surface attachment and the mixed suspension was stirred overnight at room temperature. The surface modified TiNT was centrifuged and carefully washed with toluene, ethanol, and acetone. The products were dried under vacuum for 4 hours.

Formation of polyelectrolyte brushes. Under an atmosphere of nitrogen, initiator modified TiNT (1.5 g) was suspended in aqueous solution containing of sodium 2-acrylamido-2-methylpropane sulfonate (23 g, 200 ml) in a Schlenk flask. The mixture was degassed through 5 freeze-thaw cycles under vacuum to remove trace of oxygen and polymerized at 60°C for desired period of time. After polymerization, samples were separated by centrifugation and washed with 0.1 M HCl aqueous solution 4 times (each washing step for 30 minutes) to transfer the sodium salt to acid form. After extracting the non-attached polymers with methanol using a Soxhlet apparatus for 15 hours, the resulting white powders were dried at 80°C under vacuum overnight. Free polymers in solution were dried using lyophilizer and were used for determination of molecular weight.

Characterization. Nitrogen adsorption-desorption isotherm of TiNTs was measured at 77 K on JW-BK instrument (JWGB Sci & Tech Co., Ltd., China) after samples were degassed under vacuum overnight to remove physically adsorbed gases. Surface area, pore volume, and pore size distribution of TiNT substrates were calculated from the adsorption-desorption isotherm of nitrogen. Weight average Molecular mass of polymers was determined by gel permeation chromatography (GPC-SEC system, SUPERA water column, Agilent) calibrated with polyacrylic acid – sodium salts (PAA-10). Fourier transform infrared spectra (FTIR, Bio-Rad FTS 300) were recorded with a resolution of 4 cm⁻¹ to investigate the coupling reaction and the structure of the surface attached amino groups. Hydrodynamic diameters of TiNT and polyAMPS brushes were measured using dynamic light scattering techniques on Malvern HPPS Laser Particle Size Analyzer (Malvern, UK) with scattering angle of 90° at 25°C using He-Ne laser (633 nm). Samples for light scattering measurements were prepared by suspending the solid powders in deionized water with concentration of about 0.01 g ml⁻¹. Morphology of TiNT powders, polyAMPS grafted TiNT powders and cross-sectional morphology of formed polyAMPS brush pellet was examined using scanning electron microscopy (SEM, JEOL JSM-5610LV). The pellet for cross-sectional SEM image was first formed by compact polyAMPS brushes under pressure of 20 MPa for 3 minutes, following by fracturing the samples in liquid nitrogen. The water-uptake of pellets at different relative humidity was calculated as the ratio of the difference between the swollen and the dry weight of the membrane. The weight of swollen membrane was measured rapidly after keeping the membrane at 60°C under desired relative humidity for about 6 hrs in a temperature and relative humidity-controllable oven. For the weight of dry membrane, the measurement was made directly after drying the sample at 100°C for 2 hrs.

Proton conductivity. For proton conductivity measurements of polyAMPS brushes, samples were first compacted to pellet under pressure of about 20 MPa and the compacted pellet was sandwiched between two gold electrodes. The measurements were performed on an impedance analyzer (AutolabFG30/FRA, Eco Chemie) in the

frequency range of 10 Hz and 100 KHz and the signal amplitude of 10 mV using a homemade testing chamber with controlled temperature and relative humidity. The resistance of the compacted pellet was estimated from Cole–Cole plots and the proton conductivity was calculated using the thickness of the pellet and the electrode area.

- Srinivasan, S. *Fuel Cells: From Fundamentals to Applications* (Springer, 2006).
- Kreuer, K. D. On the development of proton conducting materials for technological applications. *Solid State Ionics* **97**, 1–15 (1997).
- Mauritz, K. A. & Moore, R. B. State of understanding of Nafion. *Chem. Rev.* **104**, 4535–4586 (2004).
- Arico, A. S. *et al.* High temperature operation of a solid polymer electrolyte fuel cell stack based on a new ionomer membrane. *Fuel Cells* **10**, 1013–1023 (2010).
- Stassi, A. *et al.* Performance comparison of long and short-side chain perfluorosulfonic membranes for high temperature polymer electrolyte membrane fuel cell operation. *J. Power Sources* **196**, 8925–8930 (2011).
- Schmidt-Rohr, K. & Chen, Q. Parallel cylindrical water nanochannels in Nafion fuel-cell membranes. *Nat. Mater.* **7**, 75–83 (2008).
- Lipman, T. E., Edwards, J. L. & Kammen, D. M. Fuel cell system economics: comparing the costs of generating power with stationary and motor vehicle PEM fuel cell systems. *Energy Policy* **32**, 101–125 (2004).
- Devanathan, R. Recent developments in proton exchange membranes for fuel cells. *Energy Environ. Sci.* **1**, 101–119 (2008).
- Peckham, T. J. & Holdcroft, S. Structure-Morphology-Property Relationships of Non-Perfluorinated Proton-Conducting Membranes. *Adv. Mater.* **22**, 4667–4690 (2010).
- Bose, S., Kuila, T., Nguyen, T. X. H., Kim, N. H., Lau, K. T. & Lee, J. H. Polymer membranes for high temperature proton exchange membrane fuel cell: Recent advances and challenges. *Prog. Polym. Sci.* **36**, 813–843 (2011).
- Yameen, B. *et al.* Hybrid Polymer–Silicon Proton Conducting Membranes via a Pore-Filling Surface-Initiated Polymerization Approach. *ACS Appl. Mater. Interf.* **2**, 279–287 (2010).
- Moghaddam, S. *et al.* An inorganic–organic proton exchange membrane for fuel cells with a controlled nanoscale pore structure. *Nat. Nanotechnol.* **5**, 230–236 (2010).
- Bavykin, D. V., Friedrich, J. M. & Walsh, F. C. Protonated Titanates and TiO₂ Nanostructured Materials: Synthesis, Properties, and Applications. *Adv. Mater.* **18**, 2807–2824 (2006).
- Thorne, A., Kruth, A., Tunstall, D., Irvine, J. T. S. & Zhou, W. Formation, structure, and stability of titanate nanotubes and their proton conductivity. *J. Phys. Chem. B* **109**, 5439–5444 (2005).
- Harris, C. S. & Rukavina, T. G. Lithium ion conductors and proton conductors: Effects of plasticizers and hydration. *Electrochim. Acta* **40**, 2315–2320 (1995).
- Paneva, D., Mespouille, L., Manolova, L., Degee, P., Rashkov, I. & Dubois, P. Preparation of well-defined poly[(ethylene oxide)-block-(sodium 2-acrylamido-2-methyl-1-propane sulfonate)] diblock copolymers by water-based atom transfer radical polymerization. *Macromol. Rapid Commun.* **27**, 1489–1494 (2006).
- Wang, X. E., Tang, H. L. & Pan, M. Perfluorosulfonic polymer electrolyte membranes prepared from alkaline-ion-assisted heat treatment. *J. Membr. Sci.* **379**, 106–111 (2011).
- Li, Q., Xiao, C., Zhang, H. N., Chen, F. T., Fang, P. F. & Pan, M. Polymer electrolyte membranes containing titanate nanotubes for elevated temperature fuel cells under low relative humidity. *J. Power Sources* **196**, 8250–8256 (2011).
- Schimmel, M. Ph. D. Thesis, Max-Planck Institute for Polymer Research, Germany (1998).
- Zhang, H. N. & Ruhe, J. Symmetric monovalent salt-induced swelling of poly(methacrylic acid) brushes. *Macromolecules* **38**, 4855–4860 (2005).
- Lei, M. *et al.* Positron annihilation lifetime study of Nafion/titanium dioxide nano-composite membranes. *J. Power Sources* **246**, 762–766 (2014).
- Sone, Y., Ekdunge, P. & Simonsson, D. Proton conductivity of Nafion 117 as measured by a four-electrode AC impedance method. *J. Electrochem. Soc.* **143**, 1254–1259 (1996).
- Yamada, M., Wei, M. D., Honma, I. & Zhou, H. S. One-dimensional proton conductor under high vapor pressure condition employing titanate nanotube. *Electrochem. Commun.* **8**, 1549–1552 (2006).
- Colomer, M. T. Nanoporous anatase thin films as fast proton-conducting materials. *Adv. Mater.* **18**, 371–374 (2006).
- Li, Q. F., He, R. H., Jensen, J. O. & Bjerrum, N. J. Approaches and recent development of polymer electrolyte membranes for fuel cells operating above 100°C. *Chem. Mater.* **15**, 4896–4915 (2003).
- Prucker, O. & Ruhe, J. Synthesis of poly(styrene) monolayers attached to high surface area silica gels through self-assembled monolayers of azo initiators. *Macromolecules* **31**, 592–601 (1998).

Acknowledgments

This work was financially supported by the National Natural Science Foundation of China (No. 51372192), the Major State Basic Research Development Program of China “973 Project” (Grant No.: 2012CB215504), the National Hi-Tech R&D Program of China



(2014AA052501), and Open Foundation from State Key Laboratory of Advanced Technology for Materials Synthesis and Processing of WHUT (2014-KF-14).

Author contributions

H.N.Z. and M.P. directed the project; H.N.Z. and H.L.T. wrote the paper; J.F. and Y.Q.H. performed the synthesis of materials; J.F., Z.K.T. and Y.Q.H. carried out the electrochemical experiments; H.L.T. and H.N.Z. analyzed the data; all authors involved the discussion of the results and paper structure.

Additional information

Competing financial interests: The authors declare no competing financial interests.

How to cite this article: Feng, J. *et al.* Proton conduction of polyAMPS brushes on titanate nanotubes. *Sci. Rep.* 4, 6225; DOI:10.1038/srep06225 (2014).



This work is licensed under a Creative Commons Attribution-NonCommercial-ShareAlike 4.0 International License. The images or other third party material in this article are included in the article's Creative Commons license, unless indicated otherwise in the credit line; if the material is not included under the Creative Commons license, users will need to obtain permission from the license holder in order to reproduce the material. To view a copy of this license, visit <http://creativecommons.org/licenses/by-nc-sa/4.0/>